Molecular Biology of the Cell
Vol. 11, 3573–3587, October 2000

Phosphorylation-dependent Localization of Microtubule-associated Protein MAP2c to the Actin Cytoskeleton[V]

Rachel S. Ozer and Shelley Halpain*

Department of Cell Biology, The Scripps Research Institute, La Jolla, California 92037

Submitted February 17, 2000; Revised May 15, 2000; Accepted July 25, 2000
Monitoring Editor: Thomas D. Pollard

Microtubule-associated protein 2 (MAP2) is a neuronal phosphoprotein that promotes net microtubule growth and actin cross-linking and bundling in vitro. Little is known about MAP2 regulation or its interaction with the cytoskeleton in vivo. Here we investigate the in vivo function of three specific sites of phosphorylation on MAP2. cAMP-dependent protein kinase activity disrupts the MAP2–microtubule interaction in living HeLa cells and promotes MAP2c localization to peripheral membrane ruffles enriched in actin. cAMP-dependent protein kinase phosphorylates serines within three KXGS motifs, one within each tubulin-binding repeat. These highly conserved motifs are also found in homologous proteins tau and MAP4. Phosphorylation at two of these sites was detected in brain tissue. Constitutive phosphorylation at these sites was mimicked by single, double, and triple mutations to glutamic acid. Biochemical and microscopy-based assays indicated that mutation of a single residue was adequate to disrupt the MAP2–microtubule interaction in HeLa cells. Double or triple point mutation promoted MAP2c localization to the actin cytoskeleton. Specific association between MAP2c and the actin cytoskeleton was demonstrated by retention of MAP2c–actin colocalization after detergent extraction. Specific phosphorylation states may enhance the interaction of MAP2 with the actin cytoskeleton, thereby providing a regulated mechanism for MAP2 function within distinct cytoskeletal domains.

INTRODUCTION

Neuronal growth and synaptic plasticity require activity-dependent remodeling of dendritic structure, events likely to involve both microtubules and actin filaments. Microtubule-associated protein 2 (MAP2) is a neuronal phosphoprotein originally isolated via its ability to copurify with microtubules through multiple polymerization cycles. MAP2 may provide one of the regulated links between extracellular signals and cytoskeletal structure. Multiple isoforms of MAP2 are encoded by a single gene, the mRNA of which undergoes differential alternative splicing to form high-molecular-weight isoforms MAP2a and MAP2b and low-molecular-weight isoforms MAP2c and MAP2d (Kalcheva *et al.*, 1995). MAP2c is expressed perinatally in rats, coincident with the period of maximal dendritic outgrowth and synaptogenesis (Riederer and Matus, 1985; Charrière-Bertrand *et al.*, 1991). Only a few CNS regions that undergo neuritigenesis throughout postnatal life, such as the olfactory bulb and the retina, continue to express MAP2c at high levels into adulthood, suggesting that MAP2c has a specific function associated with dendritic outgrowth and synaptogenesis (Tucker *et al.*, 1993).

Previous work established that the phosphorylation state of MAP2 in vivo is altered in response to neural activity, specifically the stimulation of glutamate receptors (Halpain and Greengard, 1990; Montoro *et al.*, 1993; Quinlan and Halpain, 1996). MAP2 phosphorylation is also modulated during activity-dependent changes in synaptic connectivity in vivo (Aoki and Siekevitz, 1985; Philpot *et al.*, 1997). Although these observations have been postulated to correlate with activity-dependent modifications of dendritic architecture, there has been no direct correlation of phosphorylation at specific sites with the ability of MAP2 to colocalize with cellular microtubules or actin filaments.

MAP2c binds and stabilizes microtubules in vitro, reducing microtubule dynamic instability and thereby promoting net microtubule lengthening (Gamblin *et al.*, 1996). Phosphorylation in vitro by various Ser/Thr protein kinases reduces the affinity of MAP2 for microtubules in vitro (Vallee, 1980; Yamauchi and Fujisawa, 1983; Burns *et al.*, 1984; Singh *et al.*, 1984; Hoshi *et al.*, 1988, 1992; Ainsztein and Purich,

[V] Online version of this article contains video material. Online verson available at www.molbiolcell.org.

* Corresponding author: E-mail address: shelley@scripps.edu.

Abbreviations used: A, alanine; E, glutamic acid; GFP, green fluorescent protein; MALDI, matrix-assisted laser desorption ionization; MAP2, microtubule-associated protein 2; PKA, cAMP-dependent protein kinase; S, serine; wt, wild-type.

1994; Illenberger *et al.*, 1996), and it has been widely assumed, although never proven, that this is also the case in vivo.

MAP2 binds actin filaments in vitro and several studies demonstrated that MAP2 possesses an actin filament cross-linking activity regulated by phosphorylation (Nishida *et al.*, 1981; Selden and Pollard, 1983; Sattilaro, 1986; Yamauchi and Fujisawa, 1988). Whether MAP2 interacts directly with actin filaments in vivo has never been experimentally determined. Injection of MAP2 semipurified from transfected Sf9 cells altered the morphology of a cell line lacking actin-binding protein-280, an actin cross-linking protein (Cunningham *et al.*, 1997). However, it is unclear whether this effect involved direct binding of MAP2 to actin. The binding affinity of MAP2 is lower for actin than for microtubules in vitro, and both interactions are reduced by phosphorylation in vitro (Sattilaro, 1986; Yamauchi and Fujisawa, 1988). Phosphorylation sites involved in regulation of the actin association are not known.

The large number of potential phosphorylation sites on the MAP2 molecule has hampered efforts to identify precise mechanisms of functional regulation in vivo. All isoforms of MAP2 contain three to four copies of an 18 amino-acid imperfect repeat within the C-terminal microtubule-binding region (Lewis *et al.*, 1988; Doll *et al.*, 1993; Ferhat *et al.*, 1994). Homologous sequences are found in other MAPs, including tau and MAP4 (Illenberger *et al.*, 1996). Several studies point to the functional importance of KXGS motifs found in the microtubule-binding repeats, throughout the MAP family. Serines within the KXGS motifs of MAPs have been identified as in vitro phosphorylation targets of protein kinase C, microtubule affinity-regulating kinase, and cAMP-dependent protein kinase (PKA) (Biernat *et al.*, 1993; Ainsztein and Purich, 1994; Illenberger *et al.*, 1996). These phosphorylation events reduce microtubule-binding affinity in vitro. Results described here suggest a new functional role for phosphorylation within these highly conserved motifs.

We have hypothesized that activity-dependent changes in MAP2 phosphorylation represent a mechanism for the construction and remodeling of dendritic structure via modulation of the interaction of MAP2 with microtubules and actin filaments (Halpain and Greengard, 1990; Quinlan and Halpain, 1996). The present study sought to investigate whether PKA activity in situ is linked to the ability of MAP2 to bind and stabilize microtubules and at what specific sites such regulation is exerted. In addition, we asked whether phosphorylation events that reduce MAP2–microtubule binding alter MAP2–actin interactions.

MATERIALS AND METHODS

Plasmid Construction and Site-directed Mutagenesis

Plasmids encoding EGFP-MAP2c as a fusion protein were derived from the previously described pET3aMAP2c (Gamblin *et al.*, 1996). The coding region for MAP2c was amplified by using primers that generate *Hin*DIII and *Bam*HI sites at the 5′ and 3′ ends, respectively. The polymerase chain reaction product was ligated into *Hin*DIII- and *Bam*HI-digested pEGFP-C-3 vector (Clontech, Palo Alto, CA). Mutation of S319, S350, and/or S382 to alanine (A) or glutamic acid (E) was carried out by using the Quik-Change mutagenesis kit (Stratagene, La Jolla, CA) and all constructs were sequenced after mutagenesis. Plasmid DNA was prepared for transfection by transformation into *Escherichia coli* XL2 Blue cells and selection for kanamycin resistance. Plasmid DNA for transfections was isolated and purified by using the Qiafilter maxiprep kit (Qiagen, Valencia, CA).

Recombinant Protein Expression, Purification, Phosphorylation, and 2-Dimensional (2-D) Phosphopeptide Mapping

Thermally stable MAP2c was isolated from *E. coli* BL21 (DE3) cells (Stratagene) as described previously (Gamblin *et al.*, 1996) with the exception that NaCl in the bacterial lysate was reduced to 150 mM. This material was further purified by ion exchange chromatography by using a 1-ml HiTrap SP cation-exchange column (Pharmacia, Piscataway, NJ), equilibrated with 50 mM sodium acetate, 1 mM $MgCl_2$, 1 mM EGTA, and 1 mM dithiothreitol, pH 5.5. Boiled and centrifuged bacterial lysate from 0.5–1 liter cultures, containing 10–20 mg of MAP2c, was loaded onto the column and the column was washed with >10 volumes of equilibration buffer with 0.15 M NaCl added. Purified MAP2c was eluted from the column by using equilibration buffer with the addition of 0.25 M NaCl. Fractions containing purified full-length MAP2c (>90%) were identified by SDS-PAGE and pooled.

For in vitro phosphorylation by PKA, MAP2c was buffer-exchanged by using a PD-10 gel filtration column (Pharmacia) into 50 mM HEPES, pH 7.4, 10 mM $MgCl_2$, 1 mM EDTA, 1 mM EGTA, 2 mM dithiothreitol, and protein concentration was determined (Coomassie Protein Plus reagent; Pierce, Rockford, IL). Phosphorylation reactions were conducted at 5 μM MAP2c, with 200 μM ATP (labeled for phosphopeptide mapping to 0.2–0.4 Ci/mmol with [γ-^{32}P]ATP [6000 Ci/mmol; New England Nuclear, Boston, MA]) and purified PKA (Pierce) 2 u/μg MAP2c. Samples were preincubated at 30°C for 5 min and reactions initiated by the addition of ATP. After specific incubation times, aliquots were withdrawn and reactions halted by addition to SDS-loading buffer (final concentration: 3% SDS, 62 mM Tris, 5% glycerol, 20 μl/ml β-mercaptoethanol) and immediate boiling for 3 min. Stoichiometry was calculated by purification of the phosphorylation reaction by SDS-PAGE, excision of the gel piece containing MAP2c, and Cerenkov counting of phosphate incorporation. Phosphopeptide mapping (2-D) was performed as described (Hemmings *et al.*, 1984) and evaluated via phosphorimager analysis by using ImageQuant software (Molecular Dynamics, Sunnyvale, CA).

Native Protein Isolation, Antibody Production, and Matrix-assisted Laser Desorption Ionization (MALDI) Mass Spectrometry

A new polyclonal antibody to MAP2c was developed by immunization of a New Zealand White rabbit with 400 μg of purified MAP2c in sterile phosphate-buffered saline (PBS) and complete Freund's adjuvant. Serum was collected weekly beginning 4 wk after the initial injection. Additional injections were administered 7 wk after the initial injection and at 6-wk intervals thereafter, containing 400 μg of MAP2c and incomplete Freund's adjuvant. The serum was designated 4170. Rat hippocampal homogenate was prepared by dissecting a postnatal day 10 rat hippocampus, sonication into 500 μl of boiling 1% SDS, and boiling for 2 min. Protein content was assayed by using bicinchoninic acid protein assay reagent (Pierce).

MAP2c was immunoprecipitated from postnatal day 10 hippocampal homogenate (200 μg) with 10 μl of 4170 serum as described previously (Halpain and Greengard, 1990). Coomassie staining of 8% polyacrylamide gels indicated that high- and low-molecular-weight MAP2s were the only proteins detectable in addition to immunoglobulin. The MAP2c gel piece was excised for mass spectrometry analysis, affording a sample of >90% pure native MAP2c for analysis.

Either recombinant or native MAP2c was prepared for MALDI mass spectrometry by dialysis of the MAP2c-containing gel piece against 2–3 liters of water for 3 h to remove SDS and salt, and incubation overnight at 37°C in 300 μl of 25 mM NH_4HCO_3 with 0.02 mol/mol sequencing grade trypsin (Promega, Madison, WI). The supernatant was removed and the gel piece extracted with 60% acetonitrile, 0.01% trifluoroacetic acid (3× 250 μl for 20 min each), and all extracts were combined with the digest and evaporated to dryness. MALDI time-of-flight reflectron mass spectrometry was performed by the Scripps Research Institute Core Facility (more information available at http://masspec.scripps.edu/instr.descrip.html). Ions were identified by using a 0.1% margin of precision in the PAWS 3.0 software and were only assigned when there was a unique peptide within MAP2c matching the observed mass.

Cell Culture, Transfection, cAMP Experiments, and Cytoplasmic Extraction

HeLa cells were obtained as a gift from Dr. K. Sullivan (The Scripps Research Institute, La Jolla, CA) and were cultured in a 37°C/5% CO_2 incubator in DMEM (Life Technologies, Gaithersburg, MD) supplemented with 10% heat-inactivated fetal bovine serum (Omega, Tarzana, CA), penicillin-streptomycin (100 U/ml), glutaMAX II (2 mM), sodium pyruvate (1 mM), and nonessential amino acids (0.1 mM) (all from Life Technologies). Samples for live-cell microscopy were seeded onto 35-mm culture dishes with a glass coverslip mounted over a hole in the bottom of the dish (Mattek Corp., Ashland, MA). Samples for immunocytochemistry were seeded onto sterile 18-mm glass coverslips in 12-well multiwell plates. Transfections were performed on cultures at ~40% confluency, by using Superfect (5 μl/μg DNA; Qiagen), 3 μg of DNA for a 35-mm dish (1.5 μg/12 well), and all experiments were performed 16–24 h after transfection. Brief forskolin treatments were performed by withdrawing medium from a 35-mm dish, adding forskolin to a final concentration of 20 μM, or adding vehicle alone (100% ethanol, 0.2% final) to the conditioned medium and returning it to the dish. Imaging was performed after a 10-min incubation in the incubator. Experiments to elevate cAMP for longer periods were performed by adding either forskolin (10 μM final) plus rolipram (20 μM final) or vehicle alone (100% ethanol, 0.2% final) to the medium immediately after transfection and incubating for 10 h. Incubation of cell cultures with these compounds at similar concentrations and for durations of up to 24 h has previously been used to elevate intracellular cAMP (Yoshioka *et al.*, 2000). Extraction was performed on the microscope stage by removing media, rinsing with PBS, adding extraction buffer (10 mM piperazine-*N*,*N*′-bis(2-ethanesulfonic acid), pH 6.8, 100 mM KCl, 300 mM sucrose, 2.5 mM $MgCl_2$, 1 mM $CaCl_2$, 0.4% Triton-X 100, and 5 μM taxol), incubating for 30 s, and rinsing with PBS.

Confocal Microscopy, Deconvolution Microscopy, and Immunocytochemistry

Fluorescence images from live and fixed cells were collected on an Olympus IX-70 microscope by using a 60× NA 1.4 PlanAPO oil immersion objective and the Olympus Fluoview scanning laser confocal microscopy system. All images were collected at zoom 2.5 by using the maximal dynamic range display parameters (0–4095); all pixels are equal to 0.15 μm and were collected at a scan speed of 46×10^{-6} s/pixel. For three-dimensional (3-D) reconstructions (Figure 3), images were collected by using a DeltaVision optical sectioning microscope (model 283; Applied Precision, Issaquah, WA) consisting of an Olympus IX-70 microscope with high-precision motorized XYZ stage, a PlanApo 60× NA 1.4 oil objective, and a Photometrics CH350L liquid-cooled charge-coupled device camera. Data were deconvolved by using DeltaVision software, softWoRx version 2.5. Movie sequences were assembled in Adobe Premiere. Transfected cells were fixed by incubation in 100% methanol at −20°C for 20 min, followed by washing in PBS (3× 5 min). After a 1-h incubation in 10% bovine serum albumin (BSA) in PBS to block

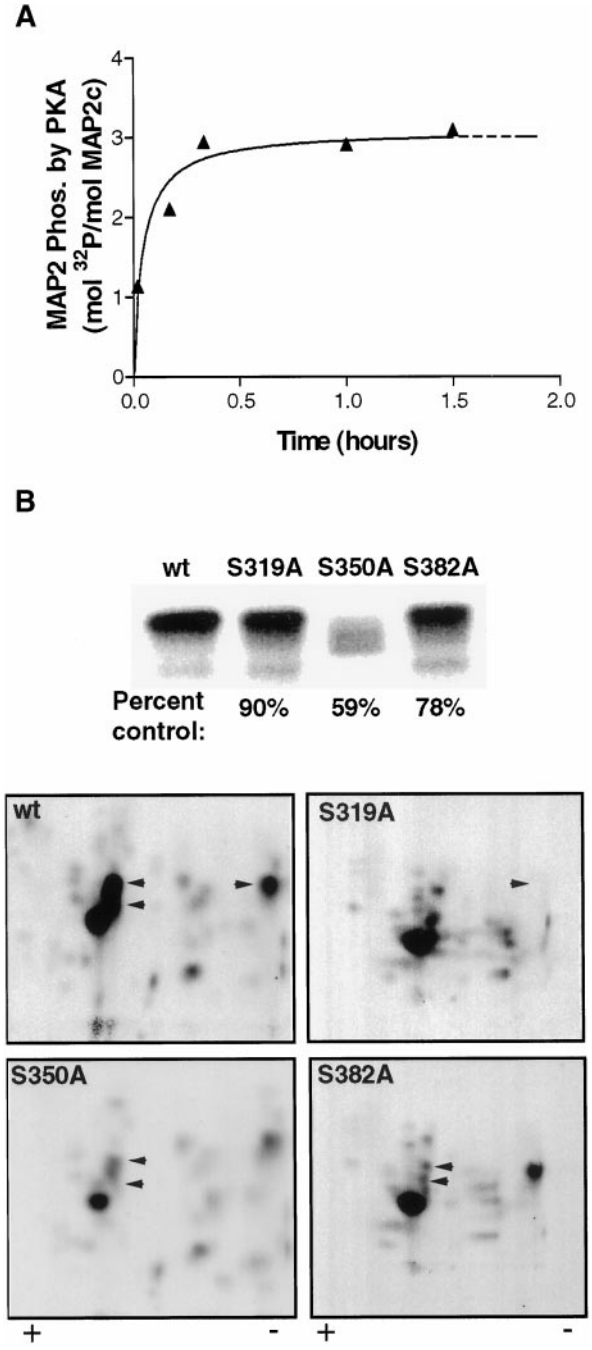

Figure 1. KXGS sites S319, S350, and S382 are major targets for in vitro phosphorylation of MAP2c by PKA. (A) Recombinant MAP2c was phosphorylated by using purified PKA in vitro as described in MATERIALS AND METHODS. Phosphorylation reached saturation within 30 min, attaining a maximum stoichiometry of 3 mol phosphate/mol MAP2c. (B) wt and mutant MAP2c were phosphorylated in the presence of PKA for 30 s and separated by SDS-PAGE (top). Excised bands were subjected to 2-D phosphopeptide mapping (bottom) by using electrophoresis in the horizontal direction, followed by ascending chromatography in the vertical direction. Mutation of S350 resulted in substantial reduction of total ^{32}P incorporation. Mutation of S319, S350, and S382 eliminated major spots from the 2-D phosphopeptide map (arrowheads).

Table 1. MAP2c phosphopeptides observed by MALDI mass spectrometry

Peptide	Predicted	Observed
In Vitro		
^{348}-CG**S**LKNIRHRPGGGRVK-^{364}	1916.2 ± 1.9	1915
^{317}-IG**S**TDNIKYQPKGGQVQIVTKK-^{338}	2482.8 ± 2.5	2480
^{380}-VG**S**LDNAHHVPGGGNVK-^{396}	1737.8 ± 1.7	1738
In Vivo		
^{339}-IDLSHVTSKCG**S**LK-^{352}	1567.7 ± 1.6	1568
^{348}-CG**S**LKNIRHRPGGGRVK-^{364}	1916.2 ± 1.9	1918
^{299}-QLRLINQPLPDLKNVK**S**K-^{316}	2184.5 ± 2.2	2186
^{302}-LINQPLPDLKNVK**S**KIG**S**TDNIKYQPK-^{328}	3212.6 ± 3.2	3212

nonspecific binding, coverslips were incubated with anti-tubulin antibody (DM1A, 1:1000; Sigma, St. Louis, MO) or anti-actin antibody (C-4, 1:500; Boehringer Mannheim, Indianapolis, IN) in 2% BSA for 1 h at 37°C. After PBS washes (3× 5 min), both primary antibodies were labeled with Cy-3-conjugated anti-mouse IgG (1:1000; Cappel, Durham, NC) for 1 h at 37°C.

Quantitative Image Analysis

To represent changes in MAP2c localization quantitatively and within multiple examples, we evaluated the coefficient of variation (SD/mean) of pixel intensity within confocal fluorescence images, restricting the analysis to the portion of the image containing a cell. We observed that in images of cells containing green flourescent protein (GFP)-MAP2c restricted to microtubules, images contained high variability in pixel intensity between the bright cytoskeleton and dark cytoplasm, a variability that is not observed if fluorescence is uniformly distributed throughout the cytosplasm. The SD of pixel intensity is therefore a representation of this variation. To correct for differences in overall brightness between images, caused by variable expression level of MAP2c, the SD was divided by mean pixel intensity, which corresponds to the average overall brightness of the image. Mean and SD of pixel intensity were collected in Adobe Photoshop 5.0 by using the raw data images and statistical analyses were performed by using Prism software (GraphPad Inc., San Diego, CA).

Subcellular Partition Assay and Immunoblotting

Comparison of expression level was performed by lysing equivalent populations of transfected cells in 1% SDS (300 μl/35-mm dish) and loading equal amounts of protein (30 μg) onto SDS-PAGE gels, transferring, and probing as described below. Subcellular partitioning was performed as described in Minotti *et al.* (1991) by lysing equivalent populations of transfected cells in a microtubule-stabilizing buffer (20 mM Tris, pH 6.8, 140 mM NaCl, 0.5% NP-40, 1 mM $MgCl_2$, 2 mM EGTA, 4 μg/ml taxol) and centrifuging to separate an insoluble cytoskeletal fraction. The supernatant was removed and the pellet was solubilized in SDS-loading buffer. Equal volumes of wild-type (wt) and mutant supernatants and solubilized pellets were separated on 8% SDS-PAGE gels and then transferred to nitrocellulose at 100 V for 2 h. Blots were probed with 4170 anti-MAP2 at 1:5000 and AP-conjugated goat anti-rabbit IgG (1:7000; Promega), or anti-tubulin B-1-5-2 (1:500; Sigma) and alkaline phosphatase-conjugated rabbit anti-mouse IgG (1:7000; Promega) in Tris-buffered saline, pH 7.35, containing 4% nonfat dry milk and 0.1% Triton X 100. Detection was performed by enhanced chemifluorescence (Amersham, Piscataway, NJ), and quantitative analysis was performed by using an FI595 fluorimager and ImageQuant software (Molecular Dynamics).

RESULTS

Identification of Phosphorylation Sites for PKA In Vitro and In Vivo

All isoforms of MAP2 bind the RII subunit of PKA and a major portion of this prominent brain kinase appears to be associated with MAP2 in brain lysates (Vallee *et al.*, 1981), via a binding site near the N terminus of the MAP2 molecule (Obar *et al.*, 1989; Rubino *et al.*, 1989). PKA phosphorylates MAP2 in vitro (Sloboda *et al.*, 1975; Theurkauf and Vallee, 1983). We therefore focused our initial studies on PKA because it is a likely regulator of endogenous MAP2 in neurons.

Specific studies of MAP2 phosphorylation and its role in regulating dendritic architecture first require the identification and functional characterization of specific amino acid residues where PKA or other cellular kinases exert regulation of the MAP2 interaction with microtubules and actin filaments.

Phosphorylation of purified recombinant MAP2c (rMAP2c) by purified PKA in vitro reaches saturation at a maximal stoichioimetry of ~3 mol phosphate/mol MAP2c after 1 h (Figure 1A). A 2-D phosphopeptide map of MAP2c phosphorylated to saturation by PKA contained multiple phosphopeptides with varying intensities, suggesting phosphate incorporation at many sites to varying stoichiometry. Very early in the time course, the kinase displayed greater apparent specificity. After only 30 s, the 2-D phosphopeptide map contained fewer spots with less variation in intensity. These early targets are likely to represent the preferred substrates for PKA on the MAP2c molecule and we therefore focused our attention on these sites.

Purified rMAP2c was briefly phosphorylated (30 s) in the presence of PKA, digested with trypsin, and the resulting mixture of peptides was subjected to MALDI mass spectrometry. Multiple phosphopeptides were observed, as well as nonphosphorylated peptides, corresponding to the majority of the MAP2c molecule. Identification of specific phosphorylation sites on each phosphopeptide was complicated in most cases by the presence of multiple potential phosphorylation sites on each peptide fragment. Phosphoamino acid analysis on rMAP2c phosphorylated for 30 s with PKA revealed no detectable levels of phosphothreonine or phosphotyrosine (our unpublished results). This allowed the unambiguous identification of phosphorylation at single

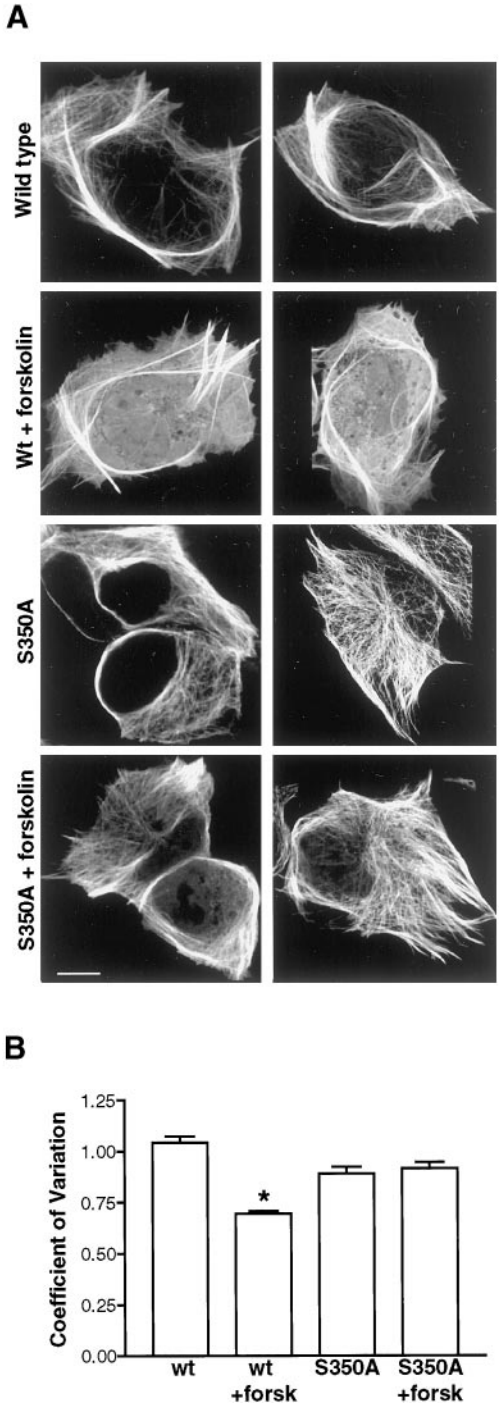

Figure 2. Effect of PKA on colocalization of MAP2c with microtubules in living HeLa cells. S350 is a major target of PKA in vivo. (A) Expression of MAP2 in HeLa cells causes remodeling of endogenous microtubule structure. Cultured HeLa cells were transiently transfected with constructs encoding wt or mutant GFP-MAP2c and incubated in the absence or presence of 20 μM forskolin for 10 min. In each row are shown two representative images of cells from each experimental group (designated at left). Bars, 10 μm. Top, HeLa cells expressing wt GFP-MAP2c that were incubated with vehicle alone contain large arrays of stable microtubules that accumulate in peripheral bundles highly enriched in GFP-MAP2c. Row 2, forskolin treatment resulted in reduced colocalization of MAP2c with microtubules and increased cytoplasmic fluorescence. Rows 3 and 4, mutation of serine 350 to alanine (S350A) eliminated forskolin-dependent changes in GFP-MAP2c localization. (B) Quantitative image analysis of control and forskolin-stimulated HeLa cells expressing MAP2c and S350A MAP2c. Mean and SD of pixel values were determined for each image and used to express the variation in fluorescence intensity within the cell as described in MATERIALS AND METHODS. Forskolin caused a substantial increase in the localization of wt GFP-MAP2c fluorescence in the cytoplasm, reflected in significantly lower pixel variation ($P < 0.0001$, Student's t test, unpaired; $n > 50$ for each group). This effect was eliminated in the S350A GFP-MAP2c ($P > 0.05$, Student's t test, unpaired, $n > 50$ for each group). Bars represent mean ± SE.

serine (S) residues present on three of the phosphopeptides. S319, S350, and S382 were thus identified as preferred targets of PKA on MAP2c (Table 1). These three residues constitute the serines of the conserved KXGS motif found in each microtubule-binding repeat.

Mass spectrometry does not provide a quantitative measure of the components of a peptide mixture and thus does not address the relative stoichiometry of phosphorylation at specific sites. We therefore evaluated this issue by using 2-D phosphopeptide maps of wt versus mutant rMAP2c phosphorylated by PKA in the presence of [γ-^{32}P]ATP. Mutation of S350 to alanine resulted in a 41% reduction in total phosphate incorporation after phosphorylation by PKA for 30 s (Figure 1B). In protein phosphorylated to saturation by PKA, the mutation of S350 to alanine reduced total phosphate incorporation by 66% (our unpublished results). Mutation of S319 or S382 to alanine resulted in 10–22% reduction in phosphate incorporation after phosphorylation by PKA for 30 s (Figure 1B).

To clarify whether S319, S350, and S382 are significant early targets of PKA in vitro, 2-D phosphopeptide mapping was performed on purified rMAP2c phosphorylated for 30 s. Mutation of S319 to alanine resulted in the elimination of one spot from the 2-D phosphopeptide map (Figure 1B). Mutation of either S350 or S382 to alanine resulted in the elimination of two spots in the central cluster of the map, suggesting either that both residues are contained within two or more peptide fragments or that mutagenesis of these residues results in altered kinase specificity at other sites.

To examine whether phosphorylation occurs at S319, S350, and S382 in vivo, antisera were raised against purified rMAP2c. Both high-molecular-weight MAP2b and low-molecular-weight MAP2c are expressed in juvenile rat hippocampus. Antiserum 4170 recognized both isoforms, similar to the commercially available monoclonal antibody HM-2 (Sigma; our unpublished results). MAP2 was immunoprecipitated from juvenile rat hippocampus by using antiserum 4170. After separation by SDS-PAGE, native MAP2c was excised from the gel and subjected to the proteolytic digestion and MALDI mass spectrometry protocol described above for recombinant MAP2c.

Peptides were observed corresponding to the majority of the MAP2c primary sequence and phosphorylation was observed at fewer sites than on MAP2c phosphorylated after brief incubation with PKA in vitro. Some phosphorylated residues were observed on multiple overlapping peptides,

facilitating identification of specific phosphorylation sites. A phosphopeptide encompassing the sequence C348-K364 contained only one possible phosphorylation site, S350 (Table 1). The additional phosphopeptide I339-K352 was also detected, confirming that phosphorylation of S350 is observed in native MAP2c. The phosphopeptide L302-K328 contained two phosphorylated residues. An additional peptide was observed with a single phosphorylated residue between Q299-K316. These data suggest that the second phosphorylation site in the L302-K328 region falls within the sequence I317-K328. Earlier work observed no detectable tyrosine phosphorylation on native MAP2 in hippocampus (Halpain and Greengard, 1990), eliminating Y325 as a likely candidate and thereby narrowing the candidate residues to either S319 or T320. Although this is not a conclusive detection of phosphorylation at S319 in the native MAP2c molecule, it is consistent with our detection of S319 phosphorylation on rMAP2c phosphorylated in vitro.

PKA Activity Regulates MAP2c Interactions with Microtubules and Actin in Living Cells

To enable observation of MAP2c localization in living cells, a plasmid was constructed encoding MAP2c as a fusion protein with GFP attached at the N terminus of MAP2c, distant from the microtubule-binding region. The GFP-MAP2c fusion protein expressed in HeLa cells colocalized with tubulin and stabilized microtubules, resulting in apparent bundles of microtubules at the periphery of the cell (Figure 2A). In mammalian cell lines, expression of MAP2 remodels endogenous microtubule structure, leading to the formation of bundles of microtubules near the perimeter of the cell (Weisshaar *et al.*, 1992). MAP2 is not thought to physically cross-link microtubules (Burgin *et al.*, 1994). Rather, the bundles are comprised of microtubules that have become hyperstabilized and aligned in parallel arrays. The cell membrane and associated cortical actin structure restrain these stabilized microtubules, causing them to bend and conform to the cell perimeter (Edson *et al.*, 1993; Tucker *et al.*, 1993). The data shown in Figure 2A are consistent with previous observations of GFP-MAP2c expressed in mammalian cell lines (Kaech *et al.*, 1996), confirming that the GFP fusion did not disrupt the MAP2c–microtubule interaction.

Although many studies have reported that phosphorylation reduces the binding of MAP2 to microtubules in vitro, there have been no previous demonstrations of stimulus-dependent distribution of MAP2c in situ. To test whether endogenous protein kinase activity regulates the interaction of MAP2c with microtubules or actin filaments, we assayed the effects of PKA stimulation on GFP-MAP2c localization in live HeLa cells.

Brief incubation of HeLa cells in the presence of 20 μM forskolin, an activator of adenylyl cyclase, significantly decreased colocalization of MAP2c with microtubules and increased GFP-MAP2c visible in the cytoplasm (Figure 2A). Quantitative image analysis of numerous cells in each treatment group ($n \geq 50$) established that the effect was statistically significant (Figure 2B). Because forskolin caused an apparent reduction in MAP2–microtubule binding in HeLa cells, we examined the hypothesis that phosphorylation at the KXGS motifs mediates this inhibition of the MAP2c–microtubule interaction. Mutation of S350 to alanine, eliminating phosphorylation at this site, was sufficient to abolish any significant effect of forskolin treatment on MAP2 localization (Figure 2, A and B). This is consistent with the in vitro data suggesting that S350 is a major target of PKA on the MAP2 molecule and suggests that S350 is likely to be a major target of PKA in living cells.[1]

The majority of the GFP-MAP2 fluorescence was retained in microtubule bundles after the 10-min forskolin treatment. This suggested that only a subpopulation of MAP2c was affected by this brief treatment. No further change in GFP-MAP2c localization was observed with incubations up to 30 min (our unpublished results). We hypothesized that MAP2c already sequestered in microtubule bundles was poorly accessible to endogenous kinases. By initiating treatments to elevate cAMP before the accumulation of MAP2c into microtubule bundles, we expected to alter the phosphorylation state of a larger fraction of overexpressed MAP2c.

To strengthen the degree of PKA activation, we used two compounds to synergistically and specifically elevate intracellular cAMP. In addition to forskolin, which activates adenylyl cyclase, we added rolipram to inhibit phosphodiesterase IV. Incubation for 10 h with a combination of forskolin (10 μM) and rolipram (20 μM), applied immediately after transfection, reduced GFP-MAP2c localization to microtubules and concomitantly raised cytoplasmic fluorescence to levels comparable to those after brief forskolin treatment. The stronger activation did not eliminate the formation of microtubule bundles, suggesting that a mixture of phosphorylated and unphosphorylated MAP2 was maintained in the cell. However, we noted a significant difference in the localization of MAP2c in these strongly cAMP-stimulated cells. In many cases, we observed the presence of GFP-MAP2c in peripheral membrane ruffles, structures that are highly enriched in actin (Figure 3B) but normally devoid of microtubules (see also Figures 8 and 9). In the absence of PKA stimulation, MAP2c was absent from peripheral membrane ruffles (Figure 3A).

MAP2 and actin thus appeared specifically enriched and partially colocalized within the peripheral membrane ruffles (Figure 3B). One possibility was that this appearance was due to thicker regions of cytoplasm, protruding upward perpendicular to the coverslip. This could cause soluble cytoplasmic proteins artifactually to appear enriched in specific locales. To determine whether this was the case, we evaluated 3-D reconstructions assembled from a z-dimensional series of deconvolved single plane images (Figure 3, ideo supplement). Neither MAP2 nor actin filled the cyto-

[1] One might expect that alanine mutation of KXGS sites would eliminate phosphorylation within living cells and promote *stronger* binding of MAP2c to microtubules. However, the low level of cytoplasmic fluorescence and high degree of microtubule bundling suggest that wt MAP2c is already binding to microtubules at maximal levels and basal phosphorylation of KXGS sites is low. In fact, there is a slight, but nonsignificant, *decrease* in the ability of S350A MAP2c to associate with microtubules (Figure 2B). This is probably because the serine-to-alanine mutation is not entirely structurally conservative. Substitution of a hydrophobic amino acid (alanine) for a polar amino acid that engages in hydrogen bonding (serine), particularly within a small domain known to mediate protein–protein interaction, may result in a slight reduction in binding affinity.

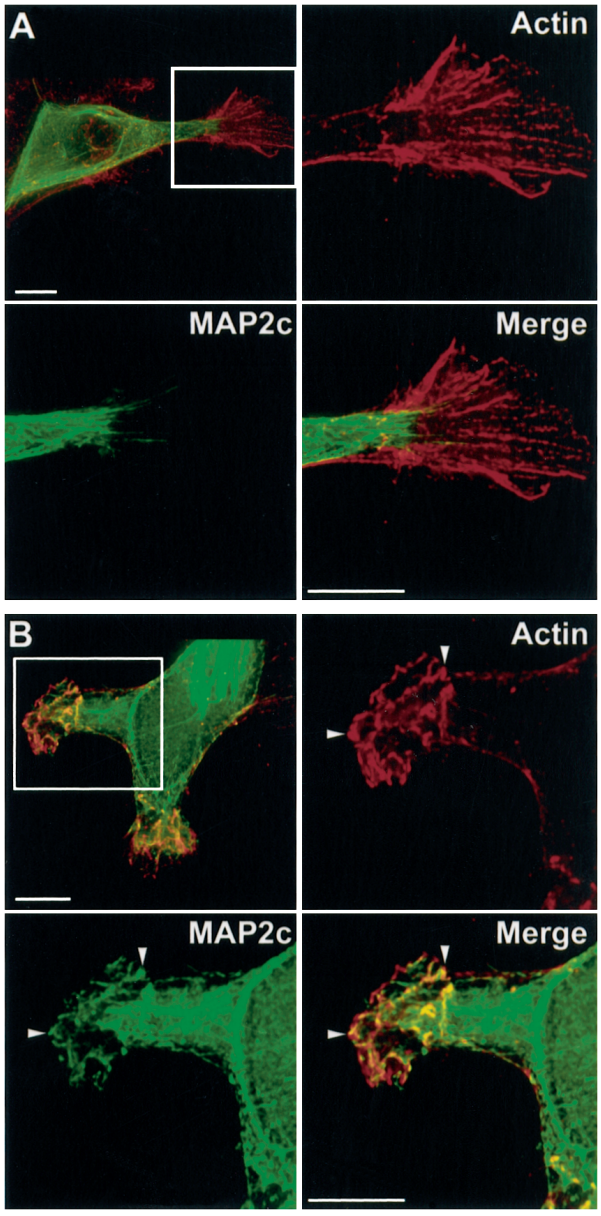

Figure 3. PKA activation promotes MAP2 association with actin. HeLa cells expressing wt GFP-MAP2c (green) were incubated with vehicle alone (A) or with 20 μM rolipram plus 10 μM forskolin for 10 h (B) as described in MATERIALS AND METHODS. Cells were fixed and immunolabeled for actin (red). Stacks of images were collected and 3-D reconstructions were created as described in MATERIALS AND METHODS. Shown are maximal projections of a series of single plane (x-y) images collected at 0.2-μm intervals in the z-dimension. The boxed regions are shown in magnified views for the actin (red), GFP-MAP2c (green), and merged images as indicated. Bars, 10 μm. (A) In control, unstimulated cells MAP2c is highly colocalized with microtubules and absent from peripheral regions enriched in actin. MAP2 is absent from actin structures within the ruffle. Video supplement OzerFig 3A.mov shows a revolving 3-D reconstruction of the merged image. (B) PKA activation promotes MAP2c–actin colocalization. Neither protein fills the cytoplasmic volume; however, GFP-MAP2c is partially colocalized within specific structures where actin is enriched (arrowheads). Video supplement OzerFig 3B.mov shows a revolving 3-D reconstruction of the merged image.

plasmic volume within the membrane ruffle. Both proteins were confined to specific domains within the ruffle, confirming that the observed colocalization was not an artifact of increased cytoplasmic volume.

KXGS Motifs Regulate MAP2c–Microtubule Interactions: Biochemical Studies

Phosphorylation states within cells are maintained via a balance of protein kinase and phosphatase activities. To clarify the functional impact of phosphorylation at a specific site, quantitative and stable modification of that site is desirable. As a mimic of constitutive phosphorylation, S319, S350, and S382 were mutated singly and in combination to glutamic acid, within the GFP-MAP2c eukaryotic expression vector. This approach allows the evaluation of the functional impact of phosphorylation at specific residues in vitro and in vivo, without the potential for modification of the sites under study due to cellular phosphatase and/or kinase activity (Bibb and da Cruz e Silva, 1997).

The transfection efficiency of all constructs was similar (at ~15% of cells transfected). Similarly, the expression levels of the S319E, S350E, S382E, S350A, S319E/S350E, and S350E/S382E GFP-MAP2c mutants displayed no significant differences from the expression level of wt GFP-MAP2c, according to quantitative immunoblot analysis (our unpublished results).

The ability of wt MAP2c and the KXGS glutamic acid mutants to bind to microtubules in living cells was evaluated biochemically by lysis of equivalent populations of transiently transfected cells in a microtubule-stabilizing buffer containing taxol. Centrifugation was used to separate the microtubule-containing fraction from the soluble fraction. Previous work demonstrated that this protocol preserves the in vivo polymerization state of the microtubules, polymer content being neither enriched nor depleted by the procedure (Minotti *et al.*, 1991). Consistent with previous observations, ~40% of the cellular tubulin was observed in the soluble fraction (Figure 4). Approximately 60% of wt MAP2c partitioned with the soluble fraction in this assay. Mutation of any KXGS site to glutamic acid significantly enriched MAP2c in the soluble fraction to 80–90% ($P < 0.01$, $n = 5$; Figure 4). These data suggest that the binding affinity of the mutants for microtubules is lower than the wt protein. No statistically significant differences were observed among the mutants ($P > 0.05$, $n = 5$) and no greater disruption was observed for double mutants than for any single mutation.

KXGS Motifs Regulate the MAP2c–Microtubule Interactions: Live-Cell Imaging

Localization of MAP2c in living cells was observed by confocal fluorescence microscopy of transiently transfected HeLa cells expressing GFP-MAP2c fusion proteins (Figure 5). As before, expression of wt MAP2c induced the apparent reorganization of endogenous microtubules into hyperstabilized bundles (Figure 5A). The S319E mutation resulted in a substantial reduction of this ability of MAP2c to remodel endogenous microtubule structure, even though this mutant retained a high degree of colocalization with microtubules (Figure 5B). The S350E mutation resulted in a further reduction of bundled microtubules and caused a visible increase in cytoplasmic fluorescence, resulting in the appearance of

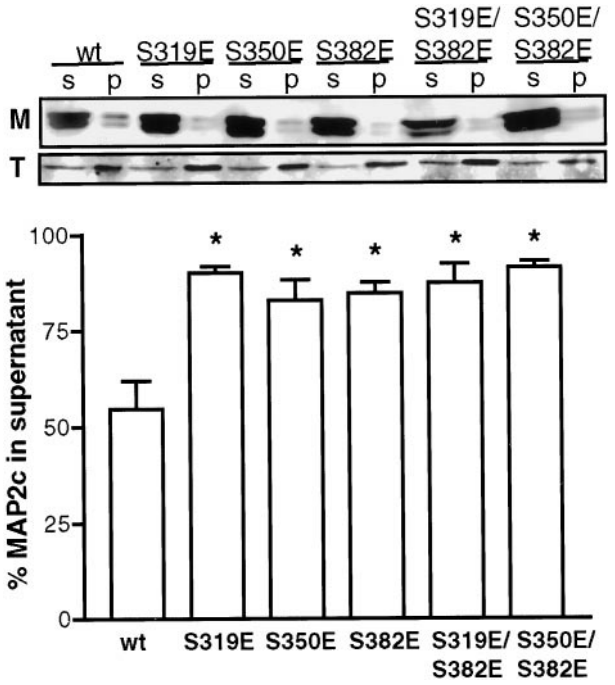

Figure 4. Mutation of KXGS serines to glutamic acid disrupts MAP2–microtubule association in living cells. Transfected HeLa cells expressing wt or mutant GFP-MAP2c were partitioned into soluble (S) and cytoskeletal pellet (P) fractions as described in MATERIALS AND METHODS. Quantitative immunoblot analysis showed that, relative to wt, each mutant form of MAP2c (M) was enriched at least 1.5-fold in the soluble fraction. Consistent with earlier work (Minotti *et al.*, 1991), ~40% of cellular tubulin (T) was observed in the soluble fraction in all cases. All mutants were significantly different from wt ($P < 0.01$) and none were significantly different from each other ($P > 0.05$, one-way ANOVA followed by Tukey's multiple comparison test, $n = 5$). Bars represent mean ± SE.

negatively outlined cytoplasmic vesicles and organelles from which MAP2c was excluded (Figure 5C). The S382E mutation also resulted in reduced microtubule bundling and enrichment of the cytoplasmic fluorescence (Figure 5D).

Quantitative image analysis was performed, as described in MATERIALS AND METHODS, on a large population of cells expressing wt GFP-MAP2c and each mutant ($n \geq 50$ in each group) to compare the level of cytoplasmic fluorescence, expressed as the coefficient of variation (SD/mean pixel intensity) (Figure 5E). Images of cells expressing wt GFP-MAP2c exhibited high variability in pixel intensity, due to the restricted localization of MAP2c to microtubules. The S319E mutation caused a statistically significant reduction in pixel variation compared with wt ($P < 0.001$), consistent with the visible reduction in intensely fluorescent bundles of microtubules. Differences between the S350E and the S382E mutants were not significant ($P > 0.05$). Mutation of S350 or S382 resulted in a reduction of pixel variation to ~50% of the wt value ($P < 0.001$), consistent with the diffuse cytoplasmic fluorescence observed. We note that all of the glutamic acid mutations resulted in significantly *more* disruption to the MAP2c–microtubule interaction than an alanine mutation.

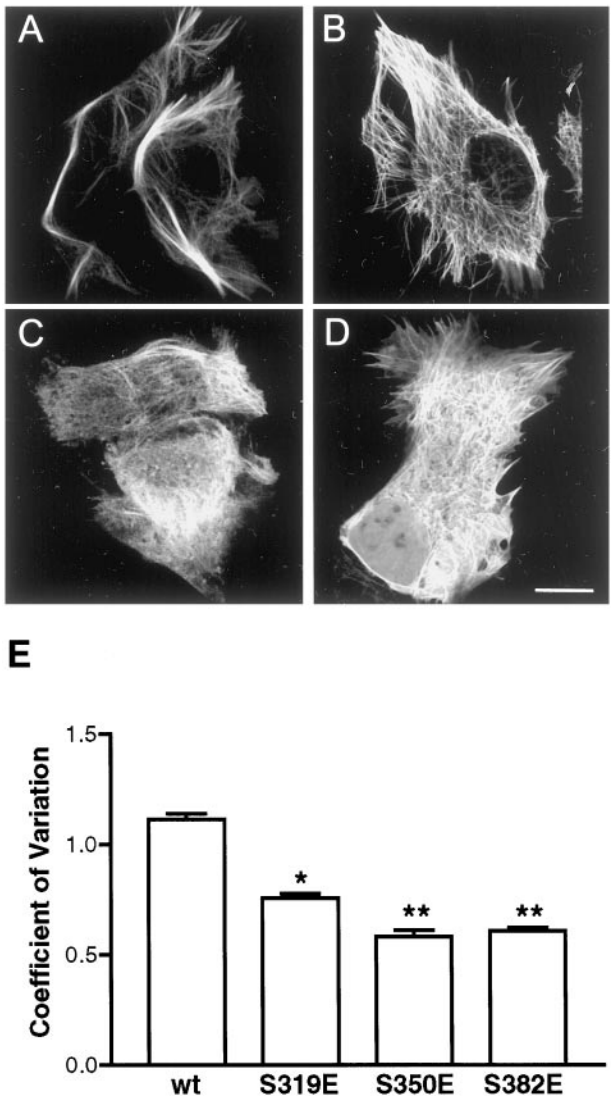

Figure 5. Single KXGS mutations reduce MAP2c–microtubule interaction. Living HeLa cells transfected to express either wt or mutant GFP-MAP2c were imaged by confocal microscopy as described in MATERIALS AND METHODS. Bar, 10 μm. (A) wt GFP-MAP2c remodels endogenous microtubules into hyperstabilized bundles. (B) S319E mutation resulted in reduced remodeling of endogenous microtubules, although MAP2c–microtubule binding appeared to be retained. (C) S350E mutation resulted in increased cytoplasmic MAP2c and the appearance of negatively outlined organelles. (D) S382E mutation resulted in increased cytoplasmic MAP2c and the appearance of negatively outlined organelles. (E) Quantitative image analysis of the effects of mutations at S319, S350, and S382. Mean and SD were determined for each image as described in MATERIALS AND METHODS and used to express the variation in pixel intensity within the cell. All mutations induced a substantial change in the localization of GFP, reflected in significantly lower pixel variation ($P < 0.001$, one-way ANOVA followed by Tukey's multiple comparison test, $n \geq 50$/group). The S319E mutant was significantly different from the S350E and S382 mutants ($P < 0.001$.); however, the S350E mutant was not significantly different from the S382E mutant ($P > 0.05$). Bars represent mean ± SE.

Images presented in the figures are representative of predominant phenotypes observed in cells expressing wt and mutant GFP-MAP2c constructs. All constructs including wt, however, do induce a certain range of microtubule phenotypes, prompting us to develop and use a quantitative assay to objectively evaluate the MAP2c–microtubule interaction.

All three KXGS motifs are targets of PKA in vitro and both S319 and S350 were observed to be phosphorylated in native tissue (Table 1). We hypothesized, therefore, that functional phosphorylation states in vivo may include simultaneous phosphorylation of multiple KXGS motifs. To evaluate the functional impact of these phosphorylation states, multiple KXGS motifs were mutated to glutamic acid to mimic specific constitutive phosphorylation. In contrast to wt GFP-MAP2c (Figure 6A), S319E/S382E (Figure 6B), S350E/S382E (Figure 6C), and S319E/S350E/S382E (Figure 6D) GFP-MAP2c all displayed reduced microtubule localization, an absence of microtubule bundles, and increased cytoplasmic fluorescence. Quantitative analysis of the coefficient of variation demonstrated that all multiple mutations were significantly different from wt ($P < 0.001$) (Figure 6E). Multiple mutations did not result in additional disruption of the MAP2c–microtubule interaction beyond that observed with the single mutations S350E or S382E. In either biochemical- or microscopy-based assays evaluating microtubule localization, no significant difference was observed between multiple mutations and the single mutations S350E and S382E ($P > 0.05$ in both assays; Figures 4 and 6).

KXGS Phosphorylation Promotes Localization to the Actin-Rich Cellular Periphery

Imaging studies suggested a potentially important difference between single and multiple KXGS mutants of MAP2c. Double and triple glutamic acid mutations in the KXGS motifs consistently promoted GFP-MAP2c localization to membrane ruffles, similar to that seen with treatments elevating intracellular cAMP (Figure 3B). This localization was almost never observed in cells expressing wt GFP-MAP2c without PKA activation, or any of the single mutant GFP-MAP2c constructs (Figures 3A, 5, and 6). Similar results were also obtained in Rat-1 fibroblasts (our unpublished results). The S350E/S382E double mutation was sufficient to promote GFP-MAP2c localization to ruffles in >95% of transfected cells (Figure 7, B–D). No additional increase in peripheral localization or altered morphology was observed with the triple mutation S319E/S350E/S382E (Figure 6D). A double mutation not including S350, S319E/S382E, also promoted GFP-MAP2c localization to ruffles in ~50% of transfected cells. wt GFP-MAP2c, in the absence of PKA stimulation (Figure 7A), was seen in cellular ruffles in <5% of transfected cells. In addition to altered MAP2c localization, the S350E/S382E mutation also occasionally promoted unusual pseudopod-like morphologies (Figure 7B), rarely seen in untransfected HeLa cells, suggesting that MAP2c may enhance lamellipodial growth. The altered phenotype was not a consequence of differential expression level; expression level in a large population of cells was similar for all constructs. Although differences in fluorescence intensity indicated variation in expression level among individual cells, S350E/S382E GFP-MAP2c was localized to peripheral ruffles to the same degree in cells with low versus high expression

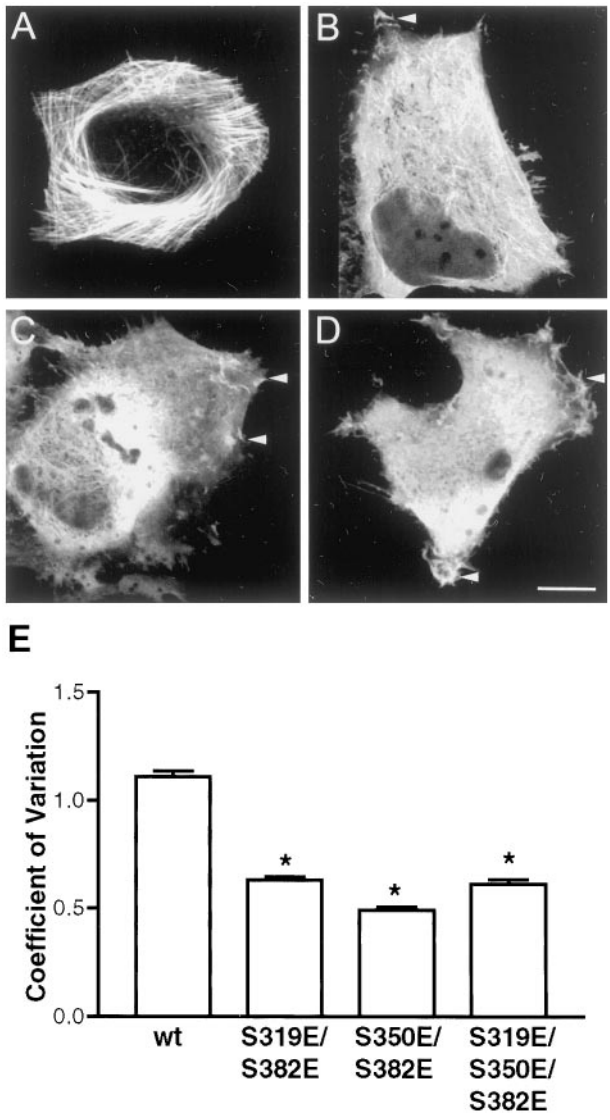

Figure 6. Multiple KXGS mutations alter subcellular localization. Living HeLa cells transfected to express either wt or mutant GFP-MAP2c were imaged by confocal microscopy as described in MATERIALS AND METHODS. Bar, 10 μm. (A) wt GFP-MAP2c remodels endogenous microtubules into hyperstabilized bundles and is excluded from the cellular periphery. (B–D) S319E/S382E (B), S350E/S382E (C), and S319E/S350E/S382E (D) mutations all resulted in increased cytoplasmic MAP2c and the appearance of negatively outlined organelles to the same degree as the S350E or S382E single mutations. Multiple mutations promoted localization to peripheral ruffles (arrowheads). (E) Quantitative image analysis of the effects of multiple mutations at S319, S350, and S382. Mean and SD were determined for each image as described in MATERIALS AND METHODS and used to express the variation in pixel intensity within the cell. All mutations induced a substantial change in the localization of GFP, reflected in significantly lower pixel variation ($P < 0.001$, one-way ANOVA followed by Tukey's multiple comparison test, $n \geq 50$/group). The multiple mutants were not significantly different from each other or from the single mutants S350E and S382E shown in Figure 5 ($P > 0.05$). Bars represent mean ± SE.

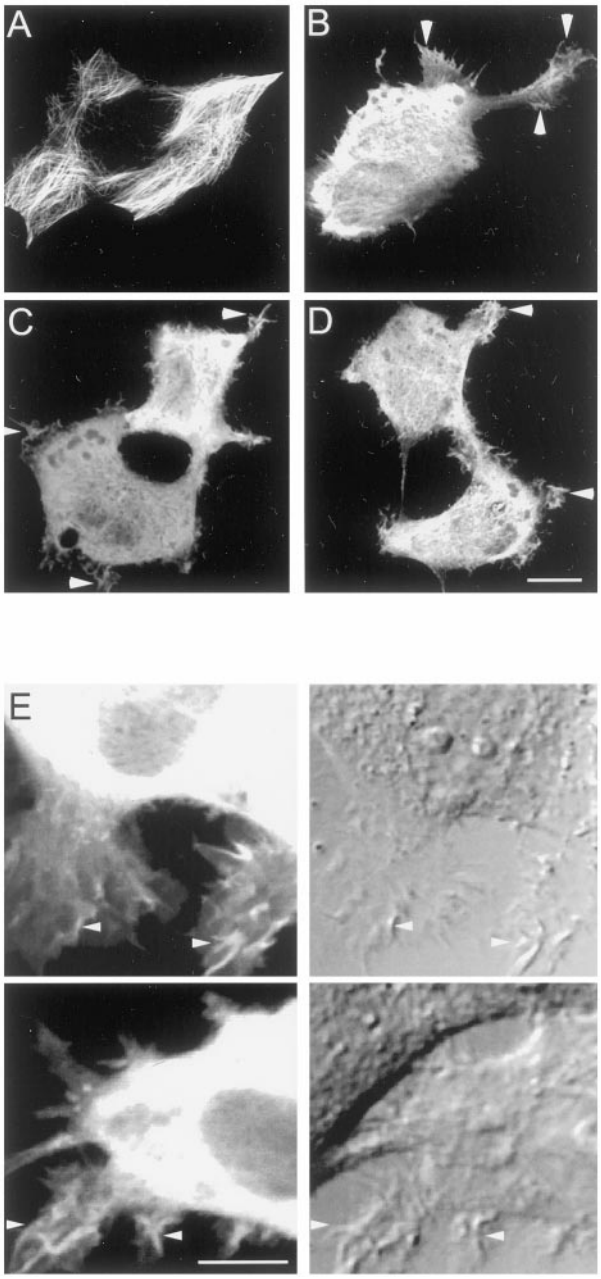

Figure 7. Mutant MAP2c localizes to motile peripheral ruffles. Living HeLa cells transfected to express either wt or mutant GFP-MAP2c were imaged by confocal microscopy as described in MATERIALS AND METHODS. Bar, 10 μm. (A) wt GFP-MAP2c is highly colocalized with microtubules and absent from the cellular periphery. (B) S350E/S382E GFP-MAP2c promotes pseudopod-like structures, which were rarely observed in untransfected HeLa cells. (C and D) Localization to ruffles is not dependent on expression level. Adjacent cells with disparate (C) or similar (D) expression levels of S350E/S382E GFP-MAP2c contain MAP2 in peripheral ruffles to a similar degree. (E) Simultaneous time-lapse differential interference contrast (right) and fluorescence (left) imaging revealed that peripheral regions enriched in S350E/S382E GFP-MAP2c (arrowheads) exhibited a high degree of motility suggestive of membrane ruffling. Shown are single frame captures from two independent time-lapse series. Bar, 10 μm.

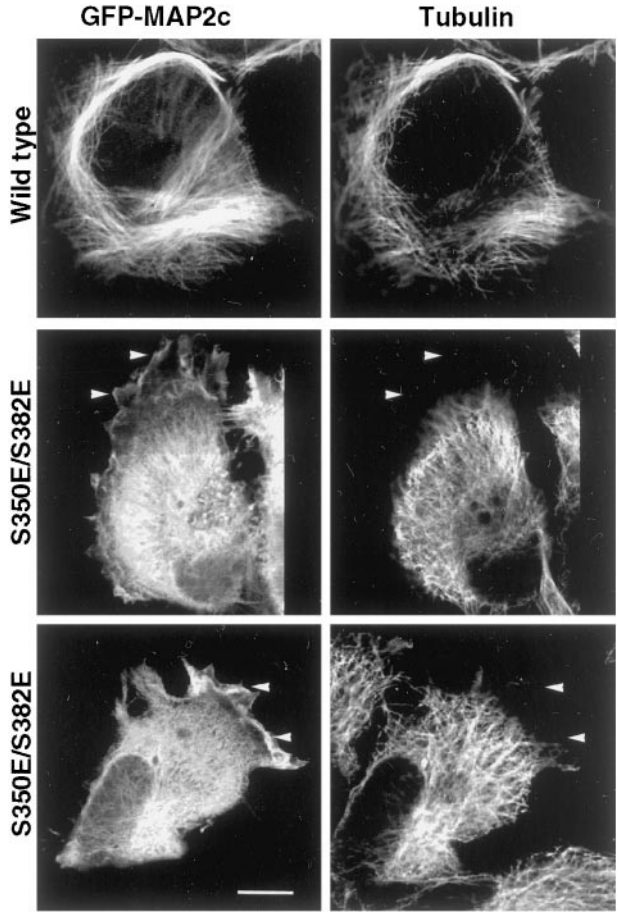

Figure 8. S350E/S382E mutant MAP2c is not restricted to microtubule-containing domains. HeLa cells expressing wt and S350E/S382E GFP-MAP2c were fixed and immunolabeled for tubulin. wt MAP2c remodeled endogenous microtubules into bundles at the periphery of the cell and MAP2c was restricted to domains of the cell also enriched in tubulin. In cells expressing S350E/S382E GFP-MAP2c, endogenous microtubules appeared similar to those in nontransfected HeLa cells because they rarely exhibited microtubule bundles and most microtubules appeared to radiate centrifugally. In addition, mutant MAP2c was enriched in peripheral structures that did not contain microtubules (arrowheads). Bar, 10 μm.

levels (cf. cells in Figure 7, C and D). Combined differential interference contrast and fluorescence time-lapse imaging confirmed that S350E/S382E GFP-MAP2c was localized to highly motile ruffle structures at the periphery of the cell (Figure 7E).

To evaluate whether these peripheral structures also contained microtubules, cells expressing wt and S350/S382 mutant GFP-MAP2c were fixed and immunolabeled for tubulin (Figure 8). wt GFP-MAP2c was localized primarily to areas of the cell also enriched in tubulin and many of the endogenous microtubules appeared in bundles. In contrast, microtubules in cells expressing S350E/S382E GFP-MAP2c were not remodeled into bundles and appeared similar to those in nontransfected cells. Mutant MAP2c was not restricted to tubulin-rich

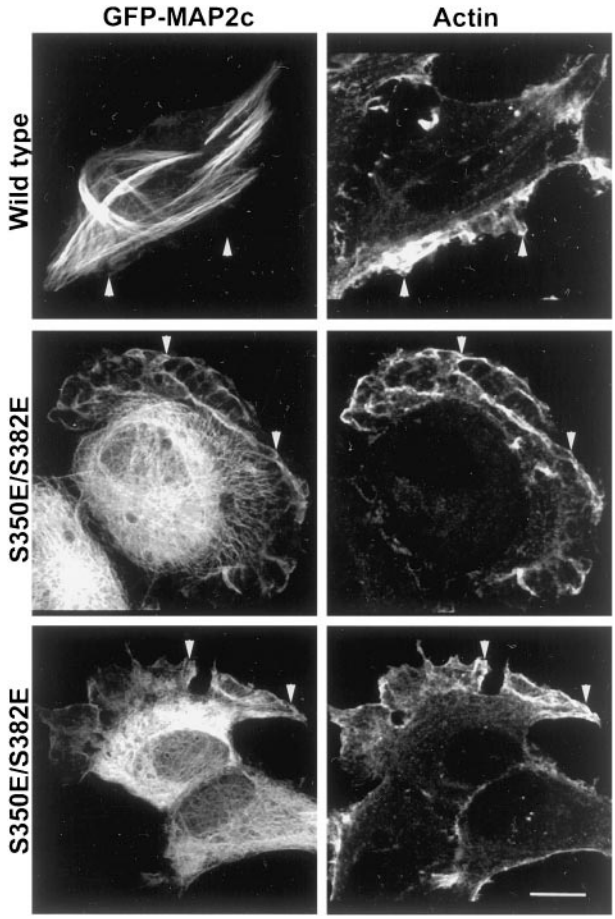

Figure 9. S350E/S382E mutant GFP-MAP2c is colocalized with actin in peripheral ruffles. HeLa cells expressing wt and S350E/S382E GFP-MAP2c were fixed and immunolabeled for actin. wt MAP2c was absent from peripheral areas of the cell and did not significantly colocalize with actin. In contrast, S350E/S382E MAP2c was enriched in peripheral ruffles that were also highly enriched in actin (arrowheads). Bar, 10 μm.

areas of the cell but was enriched in peripheral ruffles, structures that typically are highly enriched in actin filaments.

Association of MAP2c with the Actin Cytoskeleton

The appearance of MAP2c in peripheral ruffles suggested that phosphorylation events reducing the ability of MAP2 to bind microtubules might enhance its ability to interact with the actin cytoskeleton. Such a finding would be consistent with observations that MAP2 specifically binds actin filaments in vitro (Sattilaro, 1986; Cunningham *et al.*, 1997). Accordingly, we examined the ability of wt MAP2c and the S350E/S382E mutant to colocalize with actin by fixing transfected cells and immunolabeling for actin (Figure 9). As expected, in both transfected and untransfected cells, actin was enriched in areas adjacent to the plasma membrane. In regions of cells not in direct contact with neighboring cells, membrane ruffles enriched in actin were observed. As in the cAMP experiments (Figure 3), 3-D reconstruction of images of several cells confirmed the identity of these actin-rich structures as membrane ruffles (our unpublished results).

Expression of wt GFP-MAP2c did not result in detectable modifications of actin localization. Actin was not enriched in or around the microtubule bundle structures and MAP2 was absent from actin-rich areas at the cell periphery. In contrast, S350E/S382E GFP-MAP2c was enriched in peripheral areas of the cell that were also highly enriched in actin. The mutant GFP-MAP2c fusion protein colocalized with actin in numerous membrane ruffles. This result again was confirmed in 3-D reconstructions assembled from single-plane images.

To test whether the colocalization of MAP2c and actin was due to specific interaction, unfixed cells transfected with cytoplasmic GFP, wt GFP-MAP2c, or S350E/S382E GFP-MAP2c were imaged before and after extraction with a cytoskeletal-stabilizing buffer containing 0.4% Triton-X 100 (Figure 10A). Soluble, cytoplasmic GFP was almost entirely removed by the extraction and was not retained in association with any cytoskeletal structure. The microtubule-like localization of wt GFP-MAP2c was unchanged and the total fluorescence signal was only slightly diminished by this extraction procedure, indicating that wt MAP2c was tightly associated with the microtubule cytoskeleton. In contrast, extraction removed >90% of the S350E/S382E GFP-MAP2c fluorescence signal from the cell. Fluorescence was specifically retained in association with both microtubule and actin-based cytoskeletal structures, including peripheral ruffles. Interestingly, in some cells we observed the specific retention of mutant GFP-MAP2c in what appeared to be actin-based stress fibers (Figure 10B). Localization of mutant MAP2c to stress fibers was also seen in unextracted cells, although it was much more difficult to discern above the background cytoplasmic fluorescence.

DISCUSSION

MAP2 was identified more than 20 years ago as a major phosphoprotein in the brain and was shown to be a specific substrate of PKA in vitro (Sloboda *et al.*, 1975). Despite these observations, the role of PKA in regulating MAP2–cytoskeletal interactions in situ has not been examined. The present study advances our understanding of MAP2 regulation and function in three ways. First, it identifies three specific sites phosphorylated by PKA within the conserved KXGS motifs of the microtubule-binding region of MAP2. Second, it demonstrates that structural modifications designed to mimic phosphorylation at any one of these residues have a pronounced effect on the MAP2–microtubule interactions within cells. Finally, our data strongly support the novel hypothesis that phosphorylation within KXGS motifs promotes the interaction of MAP2 and the actin cytoskeleton in vivo.

KXGS Motifs and MAP2–Microtubule Interactions

All MAP2 isoforms, as well as the homologous proteins tau and MAP4, contain a conserved KXGS motif within each microtubule-binding repeat. S319, S350, and S382 are located within the KXGS motifs of MAP2c's first, second, and third repeats, respectively. Our studies strongly implicate all three KXGS motifs as important regulatory sites for MAP2c's in-

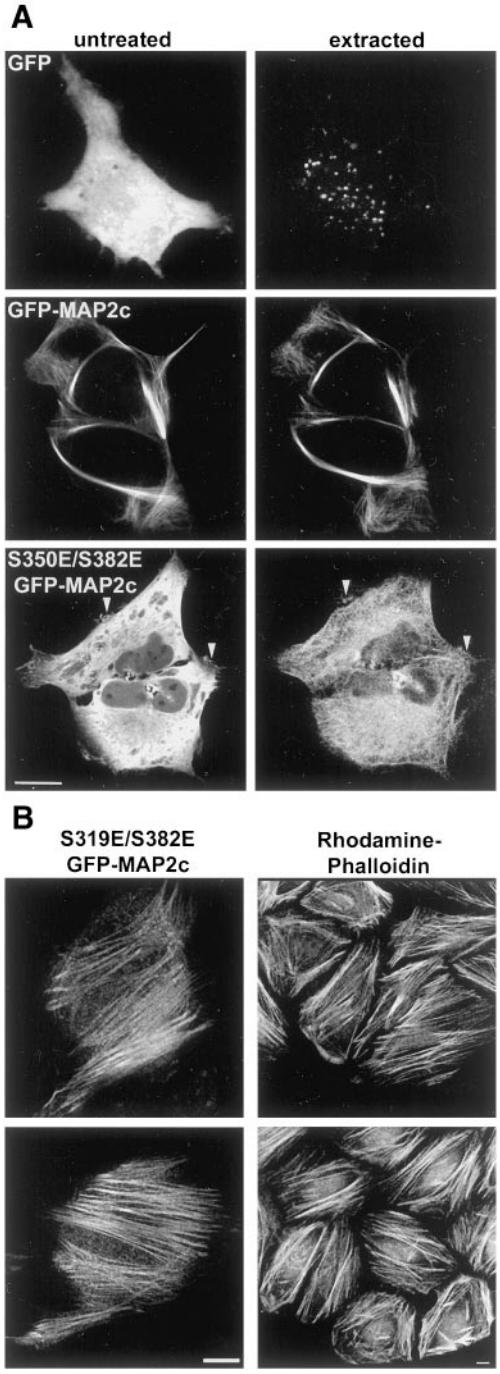

Figure 10. Specific association between mutant MAP2c and the actin cytoskeleton. (A) Unfixed HeLa cells expressing GFP, GFP-MAP2c, or S350E/S382E GFP-MAP2c were imaged before (untreated) and after extraction (extracted) with a detergent-containing buffer as described in MATERIALS AND METHODS. Virtually all soluble cytoplasmic GFP was removed by this protocol (top). The subcellular distribution and fluorescence intensity of wt GFP-MAP2c was largely unchanged by this procedure (middle). In contrast, the majority of S350E/S382E mutant GFP-MAP2c was extracted (bottom). Labeling was retained in peripheral membrane areas (arrowheads) and along filamentous structures (note that

teraction with microtubule and actin-based cytoskeletal structures.

Two previous articles describe MAP2 phosphorylation in vitro within the microtubule-binding region, but the conclusions regarding effects on microtubule binding are partly contrary to those presented here. Serines within several of the KXGS motifs of tau and MAP2c were previously identified as targets of MARK in vitro, including S350 and S319 on MAP2c (Illenberger *et al.*, 1996). In a study examining a microtubule-binding fragment of MAP2, S350 was identified as an in vitro target of protein kinase C (Ainsztein and Purich, 1994). These two previous studies both suggested that MAP2–microtubule binding is only disrupted when phosphorylation occurs within multiple repeats in the microtubule-binding domain. In contrast to these in vitro studies, our observations in living cells indicate that phosphorylation within any single KXGS motif is sufficient to strongly reduce MAP2's microtubule-binding function and eliminate microtubule bundling. Modification at multiple KXGS sites does not further impair MAP2c's ability to colocalize with microtubules but does enhance MAP2c's ability to interact with the actin cytoskeleton.

MAP2–Actin Interactions and Their Functional Implications

Further studies will be necessary to clarify the functional relationship between MAP2 and the actin cytoskeleton in vivo. Several in vitro studies have demonstrated that MAP2 binds to actin filaments and acts as an actin cross-linking protein (Selden and Pollard, 1983; Sattilaro, 1986; Cunningham *et al.*, 1997). Phosphorylation is reported to disrupt the MAP2–actin cross-linking activity, although filament binding is retained (Selden and Pollard, 1983; Sattilaro, 1986; Yamauchi and Fujisawa, 1988). A C-terminal fragment (Sattilaro, 1986) or a peptide corresponding to the second microtubule-binding repeat (Correas *et al.*, 1990) were shown to possess actin-binding activity; however, neither fragment was capable of mediating actin cross-linking. These observations suggest that the actin-binding and cross-linking activities of MAP2 are dissociable. Thus, the tubulin-binding repeats, containing the KXGS motifs, comprise a domain of the MAP2 molecule that participates in actin interaction. Actin cross-linking, on the other hand, might require multiple domains of the molecule, each subject to separate regulatory mechanisms.

wt GFP-MAP2c never appeared to localize to peripheral membrane ruffles under basal conditions. However, in cAMP-stimulated cells, wt GFP-MAP2c was often present in such ruffles, where it overlapped spatially with a small but observable fraction of the immunolabeled actin within these ruffles (Figure 3). We infer that PKA activation in HeLa cells results in substoichiometric phosphorylation on multiple KXGS motifs

Figure 10 (cont). acquisition parameters were adjusted for display purposes). Bar, 10 μm. (B) After detergent extraction, S319E/S382E GFP-MAP2c was retained in structures resembling actin-based stress fibers, which were prevalent near the bottom of the cell, closest to the glass coverslip. Left, mutant GFP-MAP2c imaged in an unfixed cell after extraction. Right, actin filaments labeled with rhodamine phalloidin in fixed HeLa cells. Bars, 10 μm.

within MAP2c, leading to interaction of this small fraction with a portion of the actin filaments. MAP2c containing Ser-to-Glu mutations within two or more KXGS motifs very strongly colocalized with a major fraction of the actin within peripheral ruffles (Figure 9). This observation is consistent with the notion that point mutations mimic constitutive phosphorylation, thereby more strongly promoting the association between actin and MAP2c. We hypothesize that in neurons phosphorylation of MAP2 on two KXGS sites may simultaneously occur under specific cellular conditions, and that this would locally promote not only its dissociation from microtubules but also its binding to F-actin.

MAP2- and tau-induced process formation in Sf9 cells has been used as a model system for studying neurite outgrowth (LeClerc *et al.*, 1996). Process outgrowth in Sf9 cells involves changes in actin organization and MAP2c localization (Boucher *et al.*, 1999). A recent study suggests that phosphorylation at two or more KXGS sites within the tubulin-binding repeats of tau, including Alzheimer's paired helical filament sites S262 and S356 (corresponding to the homologous sites S319 and S382 in MAP2c), is required for tau-dependent process formation (Biernat and Mandelkow, 1999). Consistent with the in vivo results presented here, these authors previously observed that phosphorylation at S262 is sufficient to disrupt tau–microtubule binding in vitro (Biernat *et al.*, 1993); however, elimination of single phosphorylation sites had no effect on process formation in Sf9 cells (Biernat and Mandelkow, 1999). Our data suggest a mechanism to explain these observations. We propose that two or more phosphorylation events within the KXGS motifs cause MAP2 and tau to localize to the actin cytoskeleton, where they exert functional reorganization that promotes neurite outgrowth. Antisense experiments indicate that MAP2 is required to initiate outgrowth of minor processes in cultured hippocampal neurons (Caceres *et al.*, 1992).

Several lines of evidence suggest that MAP2c may participate in actin-based cellular activities in neurons. Such a role would be consistent with the presence of MAP2 in dendritic spines (Morales and Fifkova, 1989), structures that are enriched in actin and largely devoid of microtubules. MAP2 might be specifically involved in lamellipodial formation and activity. In cultured M2 cells, microinjection of variably phosphorylated MAP2c semipurified from transfected Sf9 cells induced various morphological effects, including lamellipodia formation (Cunningham *et al.*, 1997). Our results using modified MAP2 suggest that MAP2 may promote lamellipodial extension (Figure 7B).

MAP2 and PKA

MAP2 can sequester PKA via its RII-binding domain (Vallee *et al.*, 1981; Rubino *et al.*, 1989), and recent studies suggest it might participate in other protein–protein interactions (Lim and Halpain, 2000). This emerging view of MAP2 as a multifunctional protein suggests that PKA or other kinases could regulate the translocation of MAP2 among various subcellular domains. Indeed, MAP2 might function, in part, to shuttle PKA itself, and perhaps other signaling molecules, between the microtubule and actin cytoskeletons.

Cyclic AMP pathways play essential roles in the development and plasticity of neurons. Indeed, PKA is a crucial component of the cellular substrates for learning and memory, events that are thought to involve reorganization of synaptic connections (DeZazzo and Tully, 1995; Abel and Kandel, 1998). Neurotransmitter receptor channels and transcription factors are among the identified substrates of PKA in neurons, but less is known about the precise cytoskeletal targets of PKA. Stimulation of cAMP in cultured cortical neurons was reported to arrest dendritic growth (Mattson *et al.*, 1988). Clearly, MAP2 is one attractive candidate for mediating PKA-dependent alterations in dendritic growth and structural plasticity. Our studies predict that local regulation of PKA, or other kinases capable of phosphorylating MAP2 within the microtubule-binding region, will have pronounced effects on the local function of MAP2.

ACKNOWLEDGMENTS

We thank Dr. Robley Williams Jr. for help with protein purification, Dr. Kevin Sullivan for the gift of HeLa cells, Dr. Ken Fish for assistance with 3-D image reconstruction, and Amy Batinica for initial in vitro MAP2 phosphorylation experiments. This work was supported by National Institutes of Health grant MH-50861 (S.H.). R.O. is the recipient of a predoctoral fellowship from the National Institute of Mental Health (MH-12504).

REFERENCES

Abel, T., and Kandel, E. (1998). Positive and negative regulatory mechanisms that mediate long-term memory storage. Brain. Res. Rev. *26*, 360–378.

Ainsztein, A.M., and Purich, D.L. (1994). Stimulation of tubulin polymerization by MAP-2. J. Biol. Chem. *269*, 28465–28471.

Aoki, C., and Siekevitz, P. (1985). Ontogenetic changes in the cyclic adenosine 3′,5′-monophosphate-stimulatable phosphorylation of cat visual cortex proteins, particularly of microtubule-associated protein 2 (MAP2): effects of normal and dark rearing and of the exposure to light. J. Neurosci. *5*, 2465–2483.

Bibb, J.A., and da Cruz e Silva, E.F. (1997). Identification of post-translational modification sites by site-directed mutagenesis. In: Regulatory Protein Modification: Techniques and Protocols, ed. H.C. Hemmings, Jr., Totowa, NJ: Humana Press, 275–307.

Biernat, J., Gustke, N., Drewes, G., Mandelkow, E.-M., and Mandelkow, E. (1993). Phosphorylation of Ser262 strongly reduces binding of tau to microtubules: distinction between PHF-like immunoreactivity and microtubule binding. Neuron *11*, 153–163.

Biernat, J., and Mandelkow, E.M. (1999). The development of cell processes induced by tau protein requires phosphorylation of serine 262 and 356 in the repeat domain and is inhibited by phosphorylation in the proline-rich domains. Mol. Biol. Cell *10*, 727–740.

Boucher, M., Belanger, D., Beaulieu, C., and LeClerc, N. (1999). Tau-mediated process outgrowth is differentially altered by the expression of MAP2b and MAP2c in Sf9 cells. Cell Motil. Cytoskeleton *42*, 257–273.

Burgin, K.E., Ludin, B., Ferralli, J., and Matus, A. (1994). Bundling of microtubules in transfected cells does not involve an autonomous dimerization site on the MAP2 molecule. Mol. Biol. Cell *5*, 511–517.

Burns, R.G., Islam, K., and Chapman, R. (1984). The multiple phosphorylation of the microtubule-associated protein MAP2 controls the MAP2:tubulin interaction. Eur. J. Biochem. *141*, 609–615.

Caceres, A., Mautino, J., and Kosik, K.S. (1992). Suppression of MAP2 in cultured cerebellar macroneurons inhibits minor neurite formation. Neuron *9*, 607–618.

Charrière-Bertrand, C., Garner, C., Tardy, M., and Nunez, J. (1991). Expression of various microtubule-associated protein 2 forms in the developing mouse brain and in cultured neurons and astrocytes. J. Neurochem. *56*, 385–391.

Correas, I., Padilla, R., and Avila, J. (1990). The tubulin-binding sequence of brain microtubule-associated proteins, tau and MAP-2, is also involved in actin binding. Biochem. J. *269*, 61–64.

Cunningham, C.C., LeClerc, N., Flanagan, L.A., Lu, M., Janmey, P.A., and Kosik, K.S. (1997). Microtubule-associated protein 2c reorganizes both microtubules and microfilaments into distinct cytological structures in an actin-binding protein-280-deficient melanoma cell line. J. Cell Biol. *136*, 845–857.

DeZazzo, J., and Tully, T. (1995). Dissection of memory formation: from behavioral pharmacology to molecular genetics. Trends Neurosci. *18*, 212–218.

Doll, T., Meichsner, M., Riederer, B.M., Honegger, P., and Matus, A. (1993). An isoform of microtubule-associated protein 2 (MAP2) containing four repeats of tubulin-binding motif. J. Cell Sci. *106*, 633–649.

Edson, K., Weisshaar, B., and Matus, A. (1993). Actin depolymerization induces process formation on MAP2-transfected non-neuronal cells. Development *117*, 689–700.

Ferhat, L., Ben-Ari, Y., and Khrestchatisky, M. (1994). Complete sequence of rat MAP2d, a novel MAP2 isoform. C.R. Acad. Sci. Ser. III *317*, 304–309.

Gamblin, T.C., Nachmanoff, K., Halpain, S., and Williams, R.C., Jr. (1996). Recombinant microtubule-associated protein 2c reduces the dynamic instability of individual microtubules. Biochemistry *35*, 12576–12586.

Halpain, S., and Greengard, P. (1990). Activation of NMDA receptors induces rapid dephosphorylation of the cytoskeletal protein MAP2. Neuron *5*, 237–246.

Hemmings, H.C., Jr., Nairn, A.C., and Greengard, P. (1984). DARPP-32, a dopamine- and adenosine 3′:5′-monophosphate-regulated neuronal phosphoprotein II. Comparison of the kinetics of phosphorylation of DARPP-32 and phosphatase inhibitor 1. J. Biol. Chem. *259*, 14491–14497.

Hoshi, M., Akiyama, T., Shinohara, Y., Miyata, Y., Ogawara, H., Nishida, E. and Sakai, H. (1988). Protein-kinase-C-catalyzed phosphorylation of the microtubule-binding domain of microtubule-associated protein 2 inhibits its ability to induce tubulin polymerization. Eur. J. Biochem. *174*, 225–230.

Hoshi, M., Ohta, K., Gotoh, Y., Mori, A., Murofushi, H., Sakai, H., and Nishida, E. (1992). Mitogen-activated-protein-kinase-catalyzed phosphorylation of microtubule-associated proteins, microtubule-associated protein 2 and microtubule-associated protein 4, induces an alteration in their function. Eur. J. Biochem. *203*, 43–52.

Illenberger, S., Drewes, G., Trinczek, B., Biernat, J., Meyer, H.E., Olmsted, J.B., Mandelkow, E.-M., and Mandelkow, E. (1996). Phosphorylation of microtubule-associated proteins MAP2 and MAP4 by the protein kinase $p110^{mark}$. J. Biol. Chem. *271*, 10834–10843.

Kaech, S., Ludin, B., and Matus, A. (1996). Cytoskeletal plasticity in cells expressing neuronal microtubule-associated proteins. Neuron *17*, 1189–1199.

Kalcheva, N., Albala, J., O'Guin, K., Rubino, H., Garner, C., and Shafit-Zagardo, B. (1995). Genomic structure of human microtubule-associated protein 2 (MAP-2) and characterization of additional MAP-2 isoforms. Proc. Natl. Acad. Sci. USA *92*, 10894–10898.

LeClerc, N., Baas, P.W., Garner, C.C., and Kosik, K.S. (1996). Juvenile and mature MAP2 isoforms induce distinct patterns of process outgrowth. Mol. Biol. Cell *7*, 443–455.

Lewis, S.A., Wang, D., and Cowan, N.J. (1988). Microtubule-associated protein MAP2 shares a microtubule binding motif with tau protein. Science *242*, 936–939.

Lim, R.W.L., and Halpain, S. (2000). Regulated association of microtubule-associated protein MAP2 with Src and Grb2: evidence for MAP2 as a scaffolding protein. J. Biol. Chem. *275*, 20578–20587.

Mattson, M.P., Guthrie, P.B., and Kater, S.B. (1988). Intracellular messengers in the generation and degeneration of hippocampal neuroarchitecture. J. Neurosci. Res. *21*, 447–464.

Minotti, A.M., Barlow, S.B., and Cabral, F. (1991). Resistance to antimitotic drugs in Chinese hamster ovary cells correlates with changes in the levels of polymerized tubulin. J. Biol. Chem. *266*, 3987–3994.

Montoro, R.J., Diaz-Nido, J., Avila, J., and Lopez-Barneo, J. (1993). *N*-Methyl-D-aspartate stimulates the dephosphorylation of the microtubule-associated protein 2 and potentiates excitatory synaptic pathways in the rat hippocampus. Neuroscience *54*, 859–871.

Morales, M., and Fifkova, E. (1989). Distribution of MAP2 in dendritic spines and its colocalization with actin. Cell. Tissue Res. *256*, 447–456.

Nishida, E., Kuwaki, T., and Sakai, H. (1981). Phosphorylation of microtubule-associated proteins (MAPs) and pH of the medium control interactions between MAPs and actin filaments. J. Biochem. *90*, 575–578.

Obar, R.A., Dingus, J., Bayley, H., and Vallee, R.B. (1989). The RII subunit of cAMP-dependent protein kinase binds to a common amino-terminal domain in microtubule-associated proteins 2A, 2B, and 2C. Neuron *3*, 639–645.

Philpot, B.D., Lim, J.H., Halpain, S., and Brunjes, P.C. (1997). Experience-dependent modifications in MAP2 phosphorylation in rat olfactory bulb. J. Neurosci. *17*, 9596–9604.

Quinlan, E.M., and Halpain, S. (1996). Postsynaptic mechanisms for bidirectional control of MAP2 phosphorylation by glutamate receptors. Neuron *16*, 357–368.

Riederer, B., and Matus, A. (1985). Differential expression of distinct microtubule-associated proteins during brain development. Proc. Natl. Acad. Sci. USA *82*, 6006–6009.

Rubino, H.M., Dammerman, M., Shafit-Zagardo, B., and Erlichman, J. (1989). Localization and characterization of the binding site for the regulatory subunit of type II cAMP-dependent protein kinase on MAP2. Neuron *3*, 631–638.

Sattilaro, W. (1986). Interaction of microtubule-associated protein 2 with actin filaments. Biochemistry *25*, 2003–2009.

Selden, S.C., and Pollard, T.D. (1983). Phosphorylation of microtubule-associated proteins regulates their interaction with actin filaments. J. Biol. Chem. *258*, 7064–7071.

Singh, T.J., Akatsuka, A., Huang, K.P., Murthy, A.S., and Flavin, M. (1984). Cyclic nucleotide- and Ca2+-independent phosphorylation of tubulin and microtubule-associated protein-2 by glycogen synthase (casein) kinase-1. Biochem. Biophys Res. Commun. *121*, 19–26.

Sloboda, R.D., Rudolph, S.A., Rosenbaum, J.L., and Greengard, P. (1975). Cyclic AMP-dependent endogenous phosphorylation of a microtubule-associated protein. Proc. Natl. Acad. Sci. USA *72*, 177–181.

Theurkauf, W.E., and Vallee, R.B. (1983). Extensive cAMP-dependent and cAMP-independent phosphorylation of microtubule-associated protein 2. J. Biol. Chem. *258*, 7883–7886.

Tucker, J.B., Paton, C.C., Henderson, C.G., and Mogensen, M.M. (1993). Microtubule rearrangement and bending during assembly of large curved microtubule bundles in mouse cochlear epithelial cells. Cell Motil. Cytoskeleton *25*, 49–58.

Vallee, R.B. (1980). Structure and phosphorylation of microtubule-associated protein 2 (MAP2). Proc. Natl. Acad. Sci. USA *77*, 3206–3210.

Vallee, R.B., DiBartolomeis, M.J., and Theurkauf, W.E. (1981). A protein kinase bound to the projection portion of MAP2 (microtubule-associated protein 2). J. Cell Biol. *90*, 568–576.

Weisshaar, B., Doll, T., and Matus, A. (1992). Reorganisation of the microtubular cytoskeleton by embryonic microtubule-associated protein 2 (MAP2c). Development *116*, 1151–1161.

Yamauchi, T., and Fujisawa, H. (1983). Disassembly of microtubules by the actions of calmodulin-dependent protein kinase (kinase II) which occurs only in the brain tissues. Biochem. Biophys Res. Commun. *110*, 287–291.

Yamauchi, T., and Fujisawa, H. (1988). Regulation of the interaction of actin filaments with microtubule-associated protein 2 by calmodulin-dependent protein kinase II. Biochim. Biophys. Acta *968*, 77–85.

Yoshioka, A., Yamaya, Y., Saiki, S., Kanemoto, M., Hirose, G., and Pleasure, D. (2000). Cyclic GMP/cyclic GMP-dependent protein kinase system prevents excitotoxicity in an immortalized oligodendroglial cell line. J. Neurochem. *74*, 633–640.